doi:10.1093/braincomms/fcaa019 BRAIN COMMUNICATIONS 2020: Page 1 of 14 | 1

BRAIN COMMUNICATIONS

Visual contrast sensitivity is associated with the presence of cerebral amyloid and tau deposition

Shannon L. Risacher,[1,2] Darrell WuDunn,[3] Eileen F. Tallman,[1,2] John D. West,[1,2] Sujuan Gao,[2,4] Martin R. Farlow,[2,5] Jared R. Brosch,[2,5] Liana G. Apostolova[1,2,5] and Andrew J. Saykin[1,2]

Visual deficits are common in neurodegenerative diseases including Alzheimer's disease. We sought to determine the association between visual contrast sensitivity and neuroimaging measures of Alzheimer's disease-related pathophysiology, including cerebral amyloid and tau deposition and neurodegeneration. A total of 74 participants (7 Alzheimer's disease, 16 mild cognitive impairment, 20 subjective cognitive decline, 31 cognitively normal older adults) underwent the frequency doubling technology 24-2 examination, a structural MRI scan and amyloid PET imaging for the assessment of visual contrast sensitivity. Of these participants, 46 participants (2 Alzheimer's disease, 9 mild cognitive impairment, 12 subjective cognitive decline, 23 cognitively normal older adults) also underwent tau PET imaging with [^{18}F]flortaucipir. The relationships between visual contrast sensitivity and cerebral amyloid and tau, as well as neurodegeneration, were assessed using partial Pearson correlations, covaried for age, sex and race and ethnicity. Voxel-wise associations were also evaluated for amyloid and tau. The ability of visual contrast sensitivity to predict amyloid and tau positivity were assessed using forward conditional logistic regression and receiver operating curve analysis. All analyses first were done in the full sample and then in the non-demented at-risk individuals (subjective cognitive decline and mild cognitive impairment) only. Significant associations between visual contrast sensitivity and regional amyloid and tau deposition were observed across the full sample and within subjective cognitive decline and mild cognitive impairment only. Voxel-wise analysis demonstrated strong associations of visual contrast sensitivity with amyloid and tau, primarily in temporal, parietal and occipital brain regions. Finally, visual contrast sensitivity accurately predicted amyloid and tau positivity. Alterations in visual contrast sensitivity were related to cerebral deposition of amyloid and tau, suggesting that this measure may be a good biomarker for detecting Alzheimer's disease-related pathophysiology. Future studies in larger patient samples are needed, but these findings support the power of these measures of visual contrast sensitivity as a potential novel, inexpensive and easy-to-administer biomarker for Alzheimer's disease-related pathology in older adults at risk for cognitive decline.

1 Department of Radiology and Imaging Sciences, Indiana University School of Medicine, Indianapolis, IN, USA
2 Indiana Alzheimer Disease Center, Indiana University School of Medicine, Indianapolis, IN, USA
3 Department of Ophthalmology, UF College of Medicine—Jacksonville, Jacksonville, FL, USA
4 Department of Biostatistics, Indiana University School of Medicine, Indianapolis, IN, USA
5 Department of Neurology, Indiana University School of Medicine, Indianapolis, IN, USA

Correspondence to: Shannon L. Risacher, PhD
Center for Neuroimaging,
Department of Radiology and Imaging Sciences,
Indiana Alzheimer Disease Center,

Received September 16, 2019. Revised December 07, 2019. Accepted February 20, 2020. Advance Access publication February 26, 2020

355 West 16th Street, Suite 4100,
Indianapolis, IN 46202, USA
E-mail: srisache@iupui.edu

Keywords: vision; Alzheimer's disease; amyloid; tau; mild cognitive impairment

Abbreviations: CN = cognitively normal; FDT = frequency doubling technology; LTL = lateral temporal lobe; MCI = mild cognitive impairment; MTL = medial temporal lobe; ROC = receiver operating characteristic; SCD = subjective cognitive decline; SUVR = standardized uptake value ratio.

Graphical Abstract

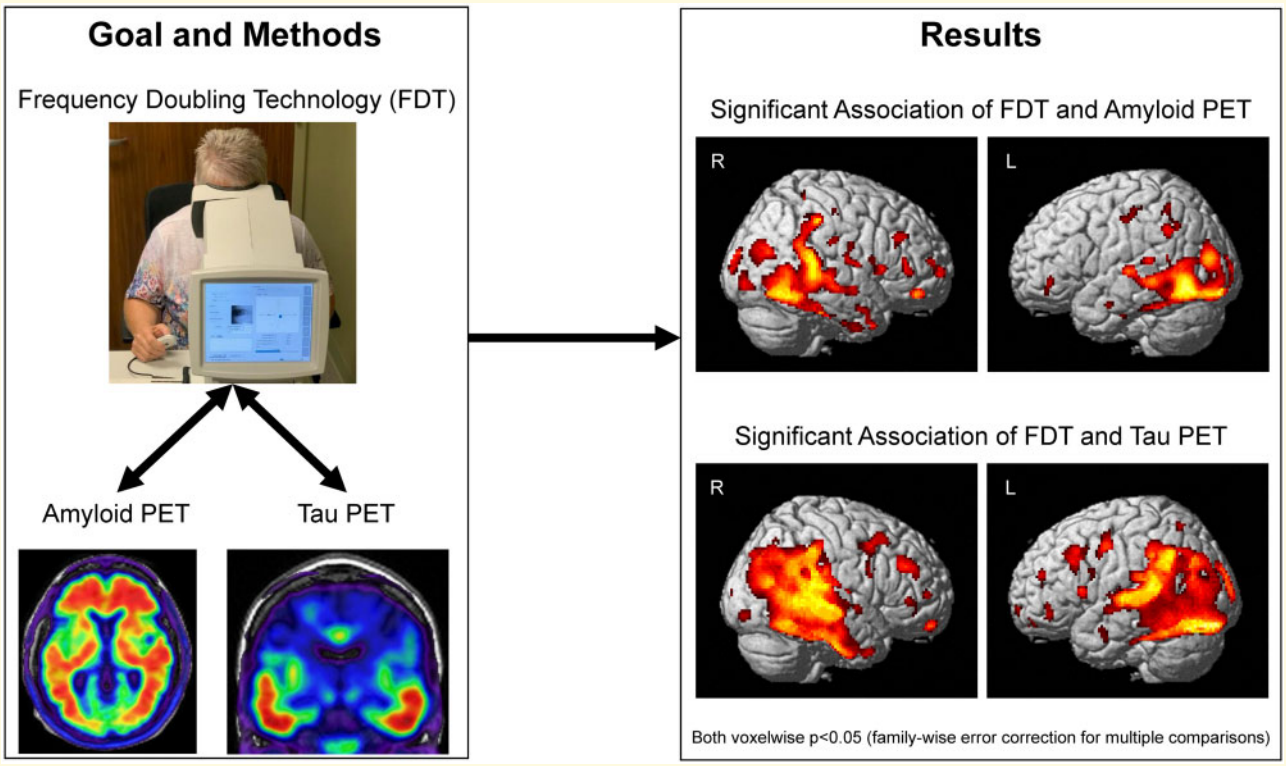

Introduction

Alzheimer's disease is a serious health concern associated with aging. The most common form of age-related dementia, Alzheimer's disease affects >5.7 million people in the USA, a number expected to rise to ~14 million in 2050 (Alzheimer's Association, 2019). Currently, no disease-modifying drugs are available to treat Alzheimer's disease. Many researchers believe that early intervention is key to the success of any future treatment. Thus, a great deal of investigation has been focused on identifying biological markers, or biomarkers, of Alzheimer's disease in early prodromal or preclinical stages of disease. Neuroimaging tools, including MRI to study brain structure and function, as well as PET imaging to measure the accumulation of the two pathological hallmarks of Alzheimer's disease, amyloid-beta plaques and tau neurofibrillary tangles, are key tools that have been identified for the early detection of Alzheimer's disease-related changes (Sperling *et al.*, 2011; Teipel *et al.*, 2015; Jack *et al.*, 2018). However, these neuroimaging methods have limited availability and are expensive, restricting their use in widespread screening. Thus, many researchers are actively engaged in studies to identify peripheral biomarkers that are cost-effective, non-invasive and easy to administer.

In addition to the well-known cognitive effects related to Alzheimer's disease, patients with Alzheimer's disease often show profound changes in sensory and perceptual processing, including in vision, smell, auditory function and motor function, among other changes (Albers *et al.*, 2015). In the visual domain, patients with Alzheimer's disease have been reported to show alterations in colour vision and pupillary response, among other changes. In addition, we and others have observed that visual contrast sensitivity, as measured using frequency doubling technology (FDT), was impaired in prodromal and mild clinical Alzheimer's disease (Cronin-Golomb *et al.*, 1991; Cormack *et al.*, 2000; Crow *et al.*, 2003; Risacher *et al.*,

2013; Valenti, 2013; Polo *et al.*, 2017) and linked to future risk to dementia (Fischer *et al.*, 2016; Ward *et al.*, 2018). Patients with Alzheimer's disease and those in prodromal stages, such as mild cognitive impairment (MCI), show thinning of retinal layers, including the retinal nerve fibre layer, and loss of retinal ganglion cells (Coppola *et al.*, 2015). Previous studies have suggested an association between retinal nerve fibre layer and other retinal layer thinning, as well as vascular changes, and amyloid deposition on PET (Snyder *et al.*, 2016; Santos *et al.*, 2018; van de Kreeke *et al.*, 2020), while others have not (Haan *et al.*, 2019; Jung *et al.*, 2019; van de Kreeke *et al.*, 2019). Some animal models of Alzheimer's disease have shown the accumulation of amyloid-beta, and its precursor, amyloid precursor protein, and hyperphosphorylated tau in the retina (Koronyo-Hamaoui *et al.*, 2011; Koronyo *et al.*, 2012; Chiasseu *et al.*, 2017; Koronyo *et al.*, 2017; Grimaldi *et al.*, 2018). A study by Koronyo-Hamaoui *et al.* (2011) demonstrated that amyloid deposition on the retina occurred concurrently with amyloid deposition in the brain. Post-mortem studies of human patients have shown mixed results, with some showing pathological amyloid and tau accumulation in the retinas of patients with Alzheimer's disease and others not observing such changes (Koronyo-Hamaoui *et al.*, 2011; Williams *et al.*, 2017; den Haan *et al.*, 2018). Recent attempts to visualize amyloid accumulation in the retina of patients with MCI and Alzheimer's disease have demonstrated sensitivity for detecting plaques that were later confirmed on autopsy (Koronyo *et al.*, 2017). Overall, these findings suggest that the assessment of retinal structure and function, as well as assessments of retinal amyloid accumulation, might be promising peripheral markers of central amyloid and tau pathology.

In the present report, we evaluated the relationship between FDT measures and cerebral amyloid and tau deposition, measured using PET. We hypothesize that contrast sensitivity will be associated with amyloid and tau deposition on PET. First, we assessed the relationship of FDT performance with amyloid and tau across the full cohort, which includes cognitively normal older adults (CN), participants with subjective cognitive decline (SCD) and patients with MCI and Alzheimer's disease. Then, to determine the sensitivity of this test to changes in participants at high risk for Alzheimer's disease, we evaluated the relationship of FDT with amyloid and tau in only SCD and MCI participants. Finally, we determined the power of FDT measures to predict amyloid or tau positivity.

Materials and methods

Participants

A total of 74 older adults (age 50+ years) were recruited from the Indiana Memory and Aging Study cohort followed by the Indiana Alzheimer Disease Center to undergo advanced PET and MRI neuroimaging and visual testing. Participants included 7 patients diagnosed with Alzheimer's disease using standard criteria (McKhann *et al.*, 2011); 16 participants diagnosed with MCI using previously established criteria (Petersen, 2004); 20 older adults characterized as SCD according to the following criteria: elevated levels of subjective memory concerns on the 20-item Cognitive Change Index, reflected as a score of $\geq$20 on the first 12 items, with or without increased levels of informant-based concerns (Jessen *et al.*, 2014; Rattanabannakit *et al.*, 2016), and without a measurable cognitive deficit; and 31 CN without significant memory concerns (12-item Cognitive Change Index total $<$20) and without a significant performance deficit on cognitive testing. The participants underwent detailed neuropsychological testing, primarily using the Uniform Dataset 3 (Weintraub *et al.*, 2018), along with the Rey Auditory Verbal Learning Test, Digit Symbol Substitution and animal and vegetable fluency. However, some individuals did not receive the Uniform Dataset 3 but instead underwent a comprehensive neuropsychological battery (Saykin *et al.*, 2006; Risacher *et al.*, 2013) with some overlapping tests (Craft Stories, animal fluency, digit span and Trail Making A and B) and other non-overlapping tests, including the California Verbal Learning Test. We combined the Rey Auditory Verbal Learning Test and California Verbal Learning Test results into a 'list learning *z*-score' for both immediate total recall and delayed recall by creating a *z*-score relative to CN participants from the larger Indiana Memory and Aging study not included in this analysis, adjusted for age, sex and years of education. Finally, all participants received either a Mini-Mental State Examination or Montreal Cognitive Assessment. The total scores from the Mini-Mental State Examination were converted to Montreal Cognitive Assessment total scores using the method described in Trzepacz *et al.* (2015).

Due to the nature of the study, participants with macular degeneration, severe cataracts, primary open-angle glaucoma, or diabetic retinopathy were excluded from the study. In addition, one participant had glaucoma in only one eye and, thus, only data from the non-glaucomatous eye were used. All analyses were run with and without those with suspected normal tension glaucoma, and all results were consistent. Thus, those with suspected normal tension glaucoma were included in the analysis to be more representative of the at-risk population.

All procedures were approved by the Indiana University School of Medicine Institutional Review Board, and informed consent was obtained according to the Declaration of Helsinki and the Belmont Report.

Amyloid PET

Amyloid PET scans were done with either [^{18}F]florbetapir (Amyvid, Eli Lilly and Co.) or [^{18}F]florbetaben

(Neuraceq, Piramal Ltd.). For the [^{18}F]florbetapir scans, ~10 mCi of [^{18}F]florbetapir was injected intravenously and, after a 50-min uptake period, participants were imaged on a Siemens mCT for 20 min using continuous listmode data acquisition. For the [^{18}F]florbetaben scans, ~8 mCi of [^{18}F]Florbetaben was injected intravenously and, after a 90-min uptake period, data were acquired for 20 min using continuous listmode acquisition on a Siemens mCT. A computed tomography scan was acquired for scatter and attenuation correction for both types of amyloid tracers. Listmode data were subsequently rebinned into four 5-min frames for both tracers, and reconstructions were conducted on the software platform (Siemens, Knoxville, TN, USA). Ordered subset expectation maximization was applied, using parameters from the Alzheimer's Disease Neuroimaging Initiative protocol (http://adni.loni.usc.edu), with corrections for scatter and random coincidence events, attenuation and radionuclide decay. Using Statistical Parametric Mapping 8, the four 5-min frames were spatially aligned to each participant's individual magnetization-prepared rapid gradient-echo scan, motion corrected, normalized to Montreal Neurologic Institute space, and averaged to create a 50- to 70-min static image for [^{18}F]florbetapir scans or a 90- to 110-min static image for [^{18}F]florbetaben scans. Then, standardized uptake value ratio (SUVR) images were created by intensity normalizing to the whole cerebellum for bother tracers. The whole cerebellum and cortical regions of interest were taken from the Centiloid project (http://www.gaain.org/centiloid-project/; Klunk *et al.*, 2015). The resulting SUVR images were converted to Centiloid units as previously described (Klunk *et al.*, 2015; Risacher *et al.*, 2017; Rowe *et al.*, 2017; Navitsky *et al.*, 2018). Finally, the [^{18}F]florbetapir and [^{18}F]florbetaben Centiloid scans were smoothed using an 8-mm full-width half maximum Gaussian kernel.

Regional [^{18}F]florbetapir and [^{18}F]florbetaben data in Centiloid units were extracted from a global cortical regions of interest from the Centiloid project (Klunk *et al.*, 2015; Risacher *et al.*, 2017; Rowe *et al.*, 2017; Navitsky *et al.*, 2018). Global cortical Centiloid units $\geq$21.02 was considered as amyloid-beta positive, as this cut-off best predicted the SUVR cut-offs produced by UC Berkeley in the Alzheimer's Disease Neuroimaging Initiative (SUVR > 1.11 for [^{18}F]Florbetapir and SUVR > 1.08 for [^{18}F]Florbetaben, data not shown).

[^{18}F]Flortaucipir PET

Of the 74 individuals, 46 individuals also underwent [^{18}F]flortaucipir scans. Briefly, ~10 mCi of [^{18}F]flortaucipir was injected intravenously; after a 75-min uptake, participants were imaged for 30 min using continuous listmode data acquisition on a Siemens mCT, rebinned into six 5-min frames and reconstructed using standard scanner software (Siemens), using ordered subset expectation maximization, with correction for scatter and random coincident events, attenuation and radionuclide decay. Using Statistical Parametric Mapping 8, the middle four 5-min frames (80–100 min) were motion corrected, normalized to Montreal Neurologic Institute space, averaged to create an 80- to 100-min static image, intensity normalized to the cerebellar crus to create SUVR images and smoothed with an 8-mm full-width half maximum Gaussian kernel.

[^{18}F]Flortaucipir SUVR was extracted from target regions known to show tau binding in Alzheimer's disease. Regions of interest were generated from participant-specific parcellations for each individual from FreeSurfer v5.1. Specifically, bilateral volume-weighted mean SUVR values were extracted from the medial temporal lobe (MTL, average of entorhinal cortex, fusiform and parahippocampal gyri), the lateral temporal lobe (LTL, average of banks of the superior temporal sulcus, inferior temporal gyri, middle temporal gyri, superior temporal gyri, transverse temporal pole) and the inferior parietal lobe.

Structural MRI

Accelerated 3-dimensional magnetization-prepared rapid gradient-echo scans were collected on a 3-T Siemens Prisma scanner using the Alzheimer's Disease Neuroimaging Initiative-2 sequence (http://adni.loni.usc.edu). Scans were coregistered to a Montreal Neurologic Institute template and segmented using Statistical Parametric Mapping 8 to create parameters for PET scan processing described above. Scans were also processed using FreeSurfer version 5.1 to create regions of interest for extracting [^{18}F]Flortaucipir SUVR and for the analysis of selected regional atrophy measures, specifically lobar (frontal, parietal, temporal and occipital) grey matter volume estimates.

Frequency doubling technology

Participants in this study underwent the FDT-2 24-2 visual field contrast sensitivity threshold examination (Welch Allyn, Skaneateles Falls, NY, USA), which evaluates 55 visual field regions in the right eye, followed by 55 regions in the left eye with 24° coverage, a stimulus size of 5°, a spatial frequency of 0.5 cycles per degree and a temporal frequency of 18 Hz (Zeppieri and Johnson, 2008). The results of this test provide a single measure of contrast sensitivity threshold (in decibels) at each of the 110 regions (55 right eye, 55 left eye) as previously described (Turpin *et al.*, 2003; McKendrick and Turpin, 2005). In addition to the threshold values for each region, a summary measure of general contrast sensitivity across the visual field is reported for each eye, referred to as the mean deviation in contrast sensitivity. A lower mean deviation represents poorer contrast sensitivity performance. In addition, because the 24-2 threshold visual field test is iterative, examination duration (in seconds)

represents a measure of contrast sensitivity performance, as more iterations (longer examination time) are needed in those with poorer contrast sensitivity. Thus, a longer examination time represents poorer contrast sensitivity performance. Finally, reliability tests are completed, including estimations of fixation errors, false positive errors and false negative errors, presented as previously described (Anderson and Johnson, 2003; Zeppieri and Johnson, 2008). Three participants had >50% errors in a single eye, thus that data were excluded from further analysis and only the eye without >50% errors was included. All visual testing was done blinded to diagnosis.

Statistical analysis

Differences between groups in demographic variables were evaluated using an analysis of variance (ANOVA) for continuous measures and chi-square for non-continuous measures in the maximal sample for each modality. Neuropsychological, clinical performance and basic imaging variables were evaluated using an analysis of covariance (ANCOVA) model, covaried for age, sex, race/ethnicity, years of education (neuropsychological tests only) and total intracranial volume (MRI variable only), using Bonferroni correction for multiple comparisons. The amyloid measures and examination duration were transformed using a natural log to create normally distributed variables. Mean deviation in contrast sensitivity was normally distributed without transformation. Tau SUVR measures were non-normal regardless of transformation type. Thus, regional tau SUVR measures were transformed using a rank-based normal transformation with Blom's formula. The associations between FDT variables and the natural log of cortical amyloid, as well as transformed MTL, LTL and inferior parietal gyri tau, were evaluated using partial Pearson correlations, adjusting for age, sex and race/ethnicity. The associations between FDT variables and lobar atrophy measures were evaluated using a partial Pearson correlation, covaried for age, sex and intracranial volume. Analyses were conducted in both the full sample and SCD and MCI only.

Next, the strongest associated FDT variable for the amyloid and tau analyses (duration and mean deviation, respectively) were entered in voxel-wise regressions and masked for grey and white matter regions, in Statistical Parametric Mapping 8 to evaluate the whole brain association pattern between these FDT measures and amyloid and tau, covaried for age, sex and race/ethnicity. A voxel-wise threshold of P-value <0.05 family-wise error-corrected for multiple comparisons and minimum cluster size (k) = 10 voxels was considered significant in the analyses across all participants and in SCD and MCI only for amyloid. The voxel-wise analyses of tau in patients with SCD and MCI only were thresholded at a cluster-wise P-value <0.05 family-wise error-corrected for multiple comparisons due to the reduced number of participants in this analysis (n = 21). Finally, the ability of the FDT variables most strongly associated to regional amyloid and tau (duration and mean deviation, respectively) to predict amyloid and tau positivity, defined as global cortical Centiloid units ≥21.02 and Braak stage ≥4 on either hemisphere (Schwarz *et al.*, 2018), respectively, was evaluated using a receiver operating characteristc (ROC) and forward conditional logistic regression models, covaried for age, sex and race/ethnicity. All analyses were done across all participants and in non-demented at-risk (SCD + MCI) participants only. In addition, all analyses were repeated after removing participants who were 3 SD above or below the whole group mean in either FDT or neuroimaging variables. Removal of these outliers did not significantly alter the relationships observed; thus, all participants are included in the analyses described below (data not shown). All non-voxel-wise statistical analyses were performed using Statistical Package for Social Sciences version 25 (https://www.ibm.com/products/spss-statistics).

Data availability

The data for this study were collected at Indiana University School of Medicine. Deidentified data specific to this analysis are available to researchers upon request through the Indiana Alzheimer Disease Center.

Results

Demographics and performance

Demographic and other sample characteristics are described in Table 1. Significant differences among groups in age, sex and race/ethnicity were observed (P < 0.05; Table 1). However, education and *APOE* genotype were not significantly different among groups. Expected impairments in cognition were observed in patients with MCI and Alzheimer's disease across cognitive domains, as well as increased self and informant complaints (most P < 0.001, Table 1). SCD participants, by design, did not show any significant differences from CN in cognitive performance but showed significantly elevated cognitive concerns on the Cognitive Change Index (all P < 0.001; Table 1). Significant or trend differences in contrast sensitivity performance were found across groups, with lower performance in patients with MCI and Alzheimer's disease (P < 0.05; Table 1). In addition, amyloid and tau deposition was significantly higher in patients with MCI and Alzheimer's disease relative to SCD and CN, while hippocampal volume was lower, as expected (P < 0.001; Table 1).

Table 1 Sample description [mean (standard deviation)]

	CN ($n = 31$)	SCD ($n = 20$)	MCI ($n = 16$)	Alzheimer's disease ($n = 7$)	*P*-value	Pair comparisons ($P < 0.05$ corrected*)
Age (years)	68.8 (4.8)	72.7 (6.4)	75.5 (8.5)	73.2 (10.6)	0.014	MCI > CN
Sex (M, F)	7, 24	9, 11	9, 7	4, 3	0.080	None
Years of education	16.9 (2.1)	17.0 (2.4)	15.4 (2.9)	17.0 (2.5)	ns	None
Race/ethnicity (% non-Hispanic Caucasian) (%)	90.3	80.0	81.3	57.1	ns	None
APOE ε4 genotype (% ε4+)[a] (%)	51.7	45.0	40.0	85.7	ns	None
MoCA total score[b]	26.6 (2.2)	26.2 (2.2)	22.4 (2.9)	15.8 (5.3)	<0.001	CN, SCD > MCI > Alzheimer's disease
CDR—memory[b]	0.05 (0.12)	0.04 (0.15)	0.55 (0.25)	0.97 (0.00)	<0.001	Alzheimer's disease > MCI > SCD, CN
CDR—global[b]	0.04 (0.12)	0.04 (0.15)	0.46 (0.13)	0.85 (0.24)	<0.001	Alzheimer's disease > MCI > SCD, CN
CDR—sum of boxes[b]	0.06 (0.23)	0.12 (0.28)	1.50 (1.25)	4.26 (1.19)	<0.001	Alzheimer's disease > MCI > SCD, CN
Digit span—forward[b,c]	7.6 (2.1)	8.9 (2.4)	7.3 (2.1)	7.2 (1.8)	ns	None
Digit span—backward[b,c]	6.7 (2.4)	7.5 (1.9)	5.3 (2.5)	5.1 (1.6)	0.040	None
Animal fluency[b,c]	22.3 (4.8)	22.6 (4.8)	17.8 (3.7)	13.1 (4.7)	<0.001	CN, SCD > MCI, Alzheimer's disease
Vegetable fluency[b,d]	16.6 (4.4)	14.9 (3.7)	10.6 (2.8)	6.4 (4.1)	<0.001	CN, SCD > MCI, Alzheimer's disease
Trail making A (s)[b,c]	33.7 (14.6)	28.5 (10.1)	39.8 (15.1)	61.5 (44.0)	0.002	Alzheimer's disease > SCD, CN
Trail making B (s)[b,e]	83.2 (43.2)	76.6 (28.8)	144.9 (102.8)	244.0 (48.6)	<0.001	Alzheimer's disease > MCI > SCD, CN
Verbal list learning—immediate (z-score)[f,g]	−0.05 (0.88)	−0.06 (0.94)	−1.26 (0.93)	−2.83 (0.72)	<0.001	CN, SCD > MCI > Alzheimer's disease
Verbal list learning—delayed (z-score)[f,g]	0.09 (0.94)	0.10 (0.98)	−1.61 (1.30)	−3.48 (1.27)	<0.001	CN, SCD > MCI > Alzheimer's disease
Craft story recall—immediate[b,h]	21.4 (5.3)	22.8 (5.2)	14.3 (5.9)	8.0 (4.2)	<0.001	CN, SCD > MCI, Alzheimer's disease
Craft story recall—delayed[b,i]	19.0 (5.2)	20.0 (5.3)	11.3 (6.1)	3.7 (2.4)	<0.001	CN, SCD, MCI > Alzheimer's disease; SCD > MCI
Benson figure copy[b,j]	15.6 (1.3)	15.1 (1.3)	15.7 (1.5)	10.5 (7.4)	<0.001	CN, SCD, MCI > Alzheimer's disease
Benson figure delayed recall[b,k]	11.9 (2.5)	12.8 (2.2)	8.1 (5.7)	0.8 (1.2)	<0.001	CN, SCD, MCI > Alzheimer's disease
MINT total score [b,k]	29.3 (2.2)	29.8 (2.4)	28.6 (3.6)	26.3 (5.7)	ns	None
Letter fluency[b,l]	28.1 (6.0)	30.9 (8.4)	27.0 (7.4)	28.7 (14.3)	ns	None
CCI self—12-item total[b,m]	16.0 (4.0)	26.6 (4.9)	34.5 (10.2)	36.3 (11.0)	<0.001	Alzheimer's disease, MCI, SCD > CN
CCI self—20-item total[b,m]	25.1 (6.0)	39.8 (7.7)	53.8 (17.2)	56.0 (17.6)	<0.001	MCI > SCD > CN; Alzheimer's disease > CN
CCI informant—12-item total[b,n]	15.2 (5.7)	16.8 (5.4)	36.8 (11.6)	45.6 (9.7)	<0.001	Alzheimer's disease, MCI > SCD, CN
CCI informant—20-item total[b,n]	24.4 (9.7)	26.3 (7.0)	58.5 (21.1)	76.7 (15.6)	<0.001	Alzheimer's disease, MCI > SCD, CN
Duration of FDT-2 examination (s)[o]	310.3 (9.5)	309.1 (7.9)	318.6 (13.7)	320.4 (16.3)	0.018	None
Mean deviation in contrast sensitivity[o]	−0.9 (2.4)	−0.9 (2.7)	−2.3 (3.8)	−4.3 (6.2)	0.088	None
Pattern standard deviation in contrast sensitivity[o]	2.9 (0.5)	3.1 (0.5)	3.7 (1.0)	3.9 (1.1)	0.005	Alzheimer's disease, MCI > CN
Cortical amyloid Centiloid[o]	2.4 (20.2)	21.5 (40.9)	54.3 (52.9)	98.2 (20.8)	<0.001	Alzheimer's disease, MCI > CN; Alzheimer's disease > SCD
Lateral temporal tau SUVR[o,p]	1.12 (0.6)	1.13 (0.6)	1.30 (0.35)	2.11 (0.50)	<0.001	CN, SCD, MCI > Alzheimer's disease
Hippocampal volume[q]	3770.4 (356.4)	3821.2 (532.2)	3518.3 (589.1)	3007.5 (521.0)	<0.001	CN, SCD, MCI > Alzheimer's disease

APOE: apolipoprotein E; CCI: Cognitive Change Index; CDR: Clinical Dementia Rating Scale; F: female; M: male; MoCA: Montreal Cognitive Assessment; ns: •••.

*Bonferroni corrected.

[a]Three participants missing (2 CN, 1 MCI).

[b]Covaried for age, sex, education and race/ethnicity.

[c]Five participants missing (1 CN, 2 SCD, 1 MCI, 1 Alzheimer's disease).

[d]Eleven participants missing (3 CN, 2 SCD, 4 MCI, 2 Alzheimer's disease).

[e]Seven participants missing (1 CN, 2 SCD, 1 MCI, 3 Alzheimer's disease).

[f]Ten participants missing (5 CN, 2 SCD, 2 MCI, 1 Alzheimer's disease).

[g]Covaried for race/ethnicity; pre-adjusted for age, sex and education.

[h]Nine participants missing (2 CN, 3 SCD, 3 MCI, 1 Alzheimer's disease).

[i]Ten participants missing (2 CN, 3 SCD, 3 MCI, 2 Alzheimer's disease).

[j]Twenty participants missing (5 CN, 5 SCD, 7 MCI, 3 Alzheimer's disease).

[k]Twenty-one participants missing (5 CN, 5 SCD, 7 MCI, 4 Alzheimer's disease).

[l]Twenty-two participants missing (5 CN, 5 SCD, 8 MCI, 4 Alzheimer's disease).

[m]Twenty-two participants missing (6 CN, 4 SCD, 8 MCI, 4 Alzheimer's disease).

[n]Twenty-six participants missing (8 CN, 7 SCD, 8 MCI, 3 Alzheimer's disease).

[o]Covaried for age, sex and race/ethnicity.

[p]Twenty-eight participants missing (8 CN, 8 SCD, 7 MCI, 5 Alzheimer's disease).

[q]Covaried for age, sex, race/ethnicity and total intracranial volume.

Contrast sensitivity associations with regional amyloid

Across all participants, significant associations between mean deviation in contrast sensitivity and cortical amyloid deposition [$r_p = -0.331$, degrees of freedom (df) = 69, $P = 0.005$; Fig. 1A] and between examination duration and amyloid deposition in the global cortex ($r_p = 0.452$, df = 69, $P < 0.001$; Fig. 1B) were observed. Within only individuals with either SCD or MCI, significant associations between mean deviation in contrast sensitivity and cortical amyloid deposition ($r_p = -0.363$, df = 31, $P = 0.038$; Fig. 1C) and between examination duration and global cortical amyloid ($r_p = 0.656$, df = 31, $P < 0.001$; Fig. 1D) were observed.

Contrast sensitivity associations with regional tau

Significant associations between mean deviation in contrast sensitivity and transformed MTL tau ($r_p = -0.499$, df = 46, $P = 0.001$; Fig. 2A), LTL tau ($r_p = -0.596$, df = 46, $P < 0.001$; Fig. 2B) and inferior parietal lobule tau ($r_p = -0.559$, df = 46, $P < 0.001$; Fig. 2C) were observed. In addition, examination duration was associated with all tau of these regions, including the MTL ($r_p = 0.422$, df = 46, $P = 0.006$; Fig. 2D), LTL ($r_p = 0.417$, df = 46, $P = 0.007$; Fig. 2E) and inferior parietal lobule ($r_p = 0.444$, df = 46, $P = 0.004$; Fig. 2F). In SCD and MCI participants only, even stronger associations were observed between mean deviation in contrast sensitivity and transformed tau deposition in the MTL ($r_p = -0.728$,

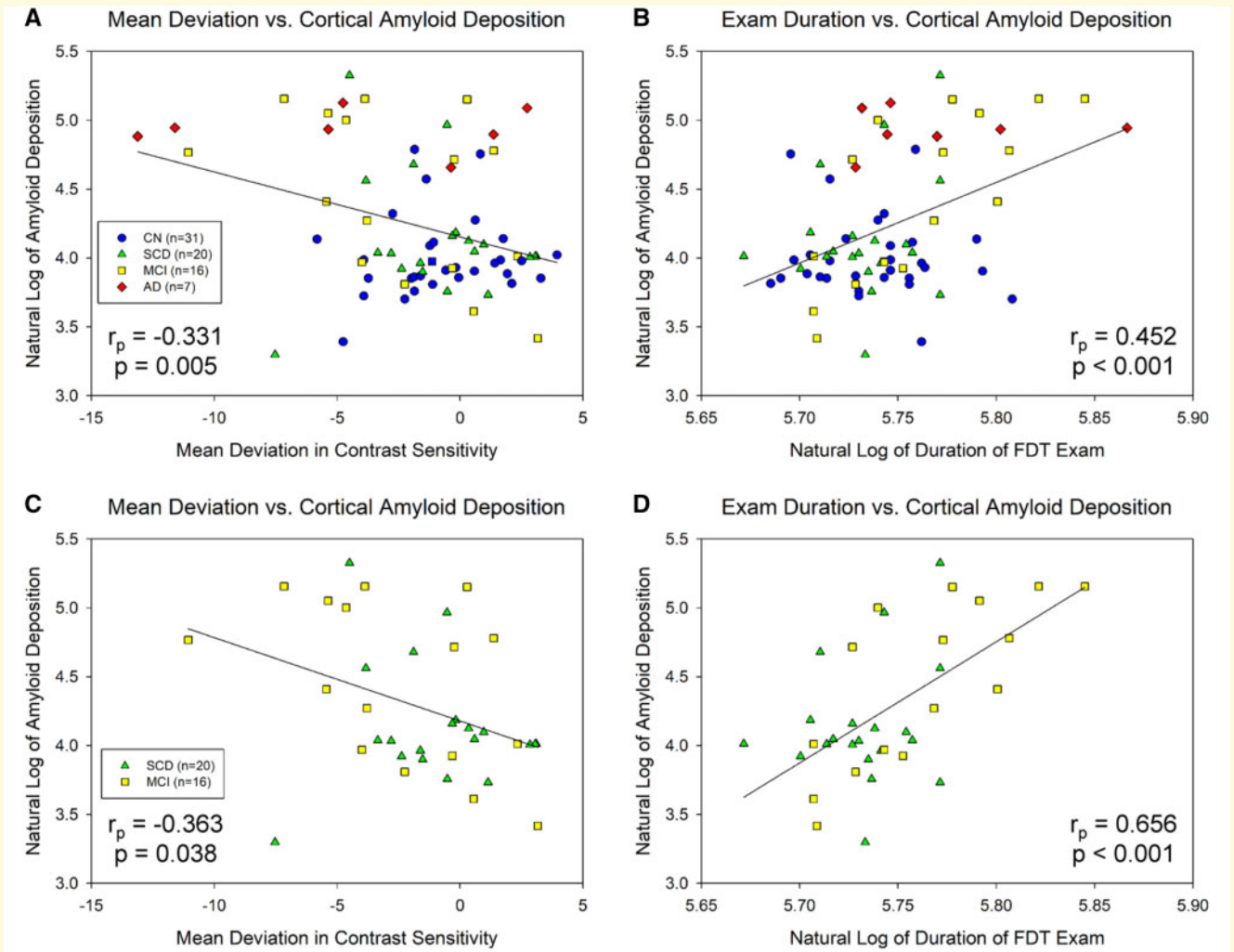

Figure 1 Visual contrast sensitivity is associated with regional cerebral amyloid deposition. Significant associations between visual contrast sensitivity, measured as mean deviation in contrast sensitivity (**A**, $P = 0.005$) and examination duration (**B**, $P < 0.001$), and cortical amyloid deposition were observed across all participants ($n = 74$). In SCD and MCI individuals only ($n = 36$), significant associations were observed between cortical amyloid and mean deviation in contrast sensitivity (**C**, $P = 0.038$), as well as examination duration (**D**, $P < 0.001$). Note that examination duration (indicated as the natural log of seconds needed to complete the examination) is a measure of contrast sensitivity performance as the test is iterative and those with poorer contrast sensitivity take longer on the examination, while lower mean deviation scores represent poorer contrast sensitivity performance. **A** and **B** include 31 CN (blue circles), 20 SCD (green triangles), 16 MCI (yellow squares), and 7 AD (red diamonds); **C** and **D** include 20 SCD (green triangles) and 16 MCI (yellow squares).

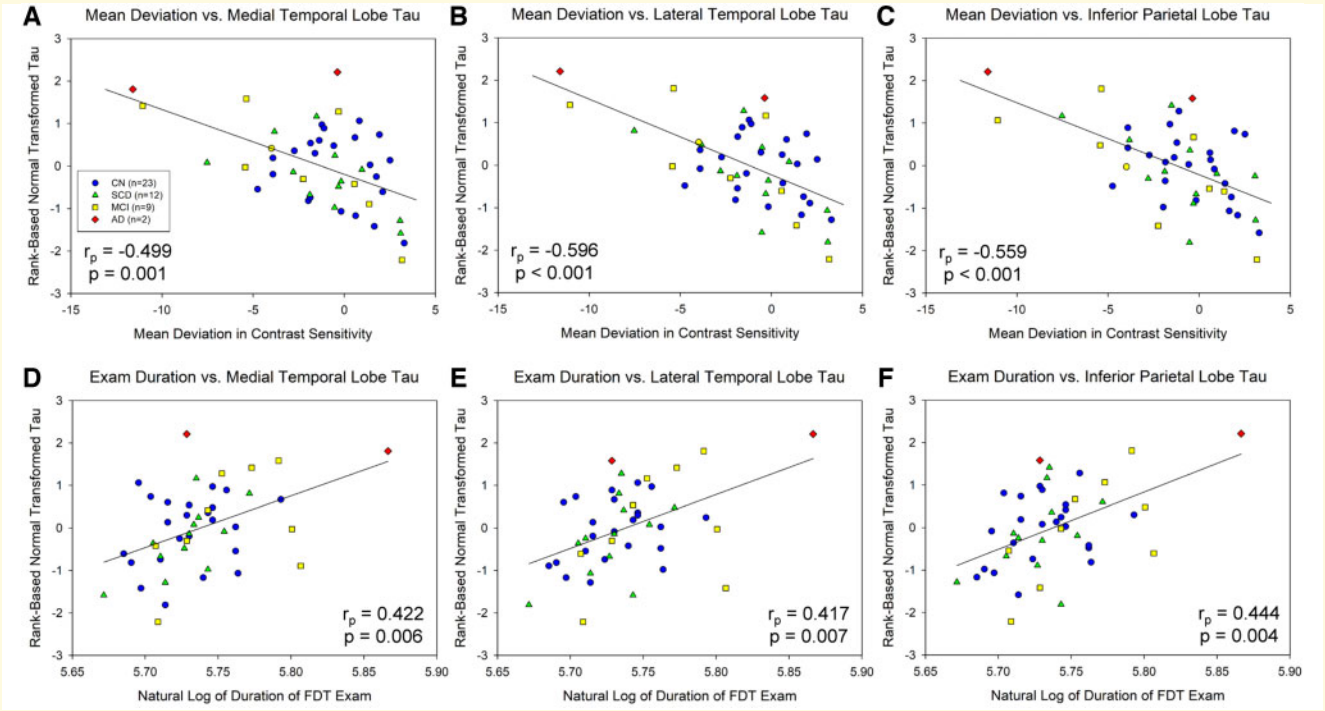

Figure 2 Visual contrast sensitivity is associated with regional cerebral tau deposition. Mean deviation in visual contrast sensitivity is significantly associated with normal transformed [^{18}F]flortaucipir SUVR in the MTL (**A**, $P = 0.001$), LTL (**B**, $P < 0.001$) and inferior parietal lobe (**C**, $P < 0.001$) across all participants ($n = 46$). In addition, examination duration is associated with normal transformed [^{18}F]flortaucipir SUVR in the MTL (**D**, $P = 0.006$), LTL (**E**, $P = 0.007$) and inferior parietal lobe (**F**, $P = 0.004$) across all participants. Note that examination duration (indicated as the natural log of seconds needed to complete the examination) is a measure of contrast sensitivity performance as the test is iterative and those with poorer contrast sensitivity take longer on the examination, while lower mean deviation scores represent poorer contrast sensitivity performance. Analysis includes 23 CN (blue circles), 12 SCD (green triangles), 9 MCI (yellow squares), and 2 AD (red diamonds).

df = 21, $P = 0.001$; Fig. 3A), LTL ($r_p = -0.775$, df = 21, $P < 0.001$; Fig. 3B) and inferior parietal lobule ($r_p = -0.641$, df = 21, $P = 0.007$; Fig. 3C). Finally, in SCD + MCI participants only, examination duration showed significant association with tau in the MTL ($r_p = 0.616$, df = 21, $P = 0.011$; Fig. 3D) and a trend for an association with tau in the LTL ($r_p = 0.446$, df = 21, $P = 0.084$; Fig. 3E) and inferior parietal lobule ($r_p = 0.429$, df = 21, $P = 0.097$; Fig. 3F).

Contrast sensitivity associations with regional atrophy

Temporal lobe grey matter volume was significantly associated with both mean deviation in contrast sensitivity ($r_p = 0.277$, $P = 0.020$; Fig. 4A) and examination duration ($r_p = -0.349$, $P = 0.003$; Fig. 4B) in the full sample of participants. Similarly, an association between temporal lobe grey matter volume and mean deviation in contrast sensitivity ($r_p = 0.418$, $P = 0.017$; Fig. 4C) and examination duration ($r_p = -0.446$, $P = 0.011$; Fig. 4D) was observed in the at-risk cohort of SCD + MCI participants only.

Voxel-wise associations of contrast sensitivity with amyloid

Amyloid in widespread regions showed association with examination duration, including in the lateral parietal and temporal lobes, the occipital lobe and the frontal lobe (Fig. 5A). When the analyses were limited to only SCD and MCI participants, more focal associations were observed between amyloid and examination duration, including in the medial and lateral parietal lobes, the temporal lobes and the occipital lobe (Fig. 5B).

Voxel-wise associations of contrast sensitivity with tau

Significant associations between mean deviation in contrast sensitivity and tau deposition in widespread regions of the posterior cortex, including the temporal and parietal lobes, the occipital lobe and a few regions in the frontal lobe (Fig. 6A), were observed. In SCD and MCI participants only, a very similar pattern of regions was significantly associated with mean deviation in contrast sensitivity, albeit at a less stringent but still significant threshold (cluster-wise versus voxel-wise $P < 0.05$ family-wise error). Specifically, mean deviation in contrast

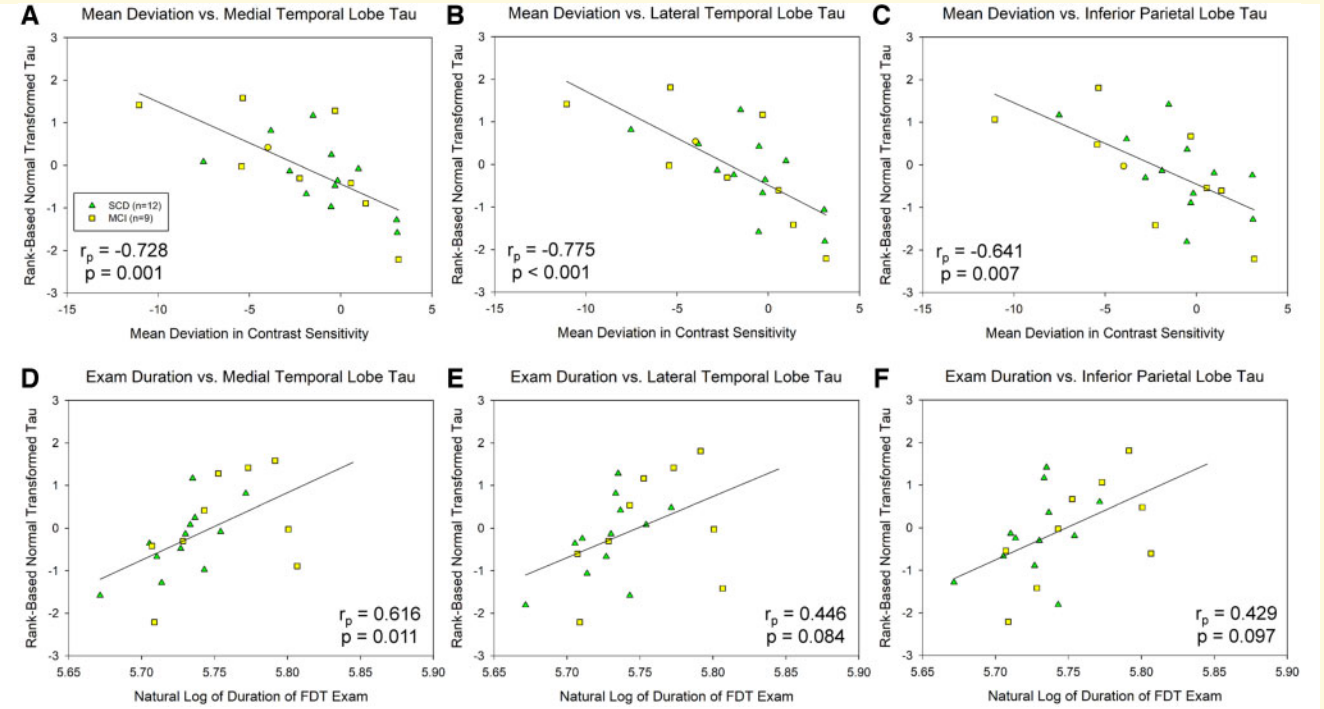

Figure 3 Visual contrast sensitivity is associated with regional cerebral tau deposition in SCD and MCI participants only. In SCD and MCI participants only ($n = 21$), the mean deviation in visual contrast sensitivity is significantly associated with normal transformed [^{18}F]flortaucipir SUVR in the MTL (**A**, $P = 0.001$), LTL (**B**, $P < 0.001$) and inferior parietal lobe (**C**, $P = 0.007$). In addition, examination duration is associated with normal transformed [^{18}F]flortaucipir SUVR in the MTL (**D**, $P = 0.011$), LTL (**E**, $P = 0.084$) and inferior parietal lobe (**F**, $P = 0.097$). Note that examination duration (indicated as the natural log of seconds needed to complete the examination) is a measure of contrast sensitivity performance as the test is iterative and those with poorer contrast sensitivity take longer on the examination, while lower mean deviation scores represent poorer contrast sensitivity performance. Analysis includes12 SCD (green triangles) and 9 MCI (yellow squares).

sensitivity was associated with tau deposition in widespread regions of the lateral temporal and parietal lobes and the occipital lobe (Fig. 6B).

Predictive modelling

Using a logistic regression model, duration of examination alone significantly predicted cerebral amyloid positivity, with an overall accuracy of 75.7% (91.7% specificity, 46.2% sensitivity; $P < 0.001$). The ROC analysis showed significant prediction of amyloid positivity by examination duration with an area under the curve of 0.731 (Fig. 7A; $P = 0.001$). In SCD and MCI participants only, examination duration, along with race/ethnicity, predicted amyloid positivity with an overall accuracy of 86.1% (95.5% specificity, 71.4% sensitivity; $P < 0.001$). In addition, the ROC analysis showed a significant prediction of amyloid positivity by examination duration with an area under the curve of 0.865 (Fig. 7C; $P < 0.001$).

Mean deviation in contrast sensitivity significantly predicted tau positivity across all participants, with an overall accuracy of 82.6% (97.1% specificity, 36.4% sensitivity; $P = 0.003$). The ROC analysis demonstrated a significant prediction of tau positivity by mean deviation in contrast sensitivity with an area under the curve of 0.735 (Fig. 7B; $P = 0.020$). The analyses in SCD and MCI participants only showed a stronger prediction of tau positivity with the combination of mean deviation in contrast sensitivity and race/ethnicity showing an overall accuracy of 90.5% (93.8% specificity, 80.0% sensitivity; $P < 0.001$) in these at-risk individuals. Finally, the ROC analysis also demonstrated a significant prediction of tau positivity by mean deviation in contrast sensitivity with an area under the curve of 0.863 (Fig. 7D; $P = 0.017$).

Discussion

In this study, we demonstrated that visual contrast sensitivity, as measured via FDT, is associated with cerebral deposition of amyloid and tau, as well as neurodegeneration, across the spectrum of Alzheimer's disease progression, as well as in at-risk groups only. Specifically, we saw strong regional and global associations of amyloid and tau, as well as temporal lobe atrophy, with visual contrast sensitivity metrics, as well as a strong predictive ability of contrast sensitivity measures to predict amyloid and tau positivity. Overall, our findings suggest that visual contrast sensitivity may be a novel, inexpensive and

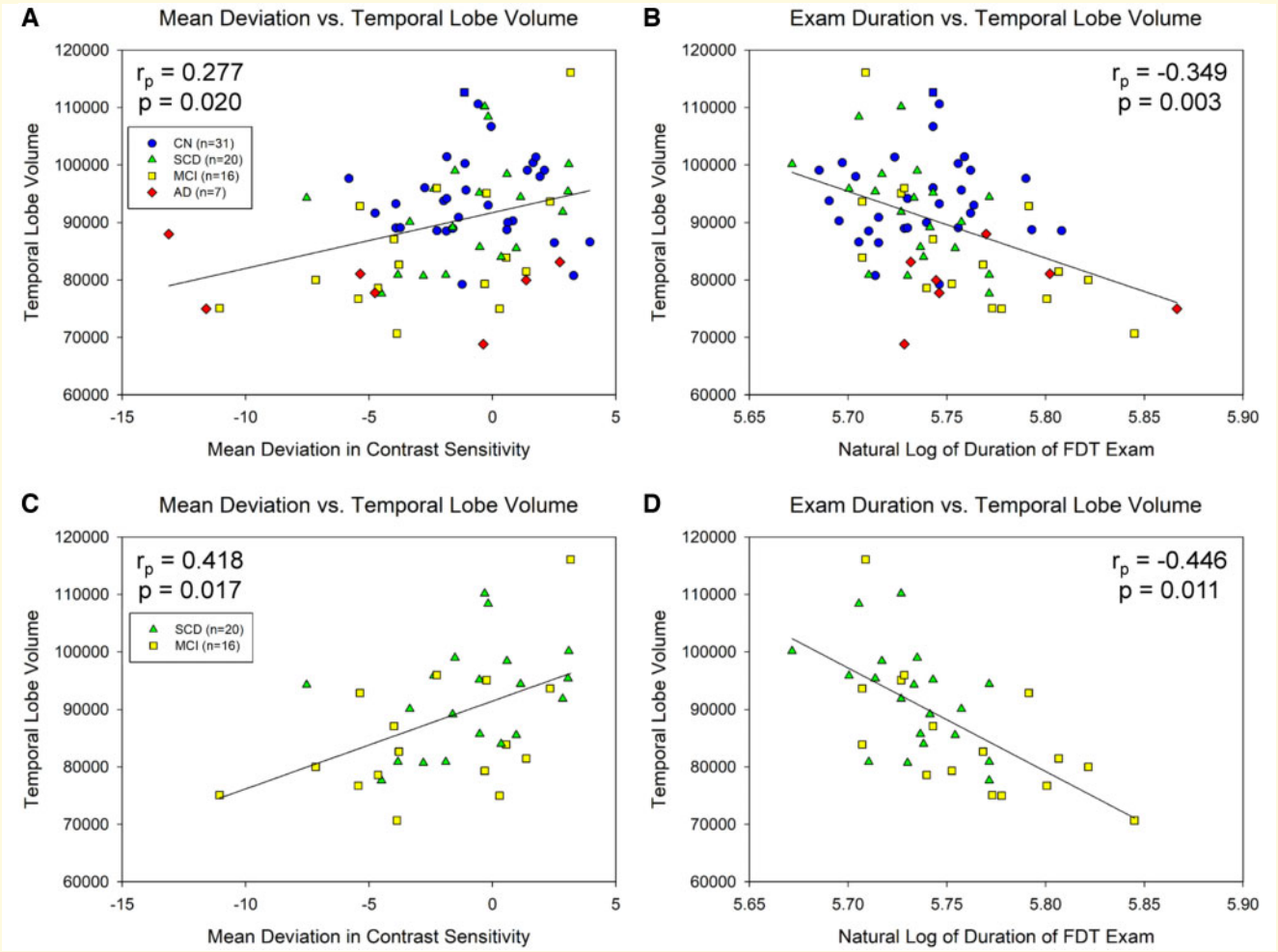

Figure 4 Visual contrast sensitivity is associated with temporal lobe volume. Significant associations between temporal lobe grey matter volume and mean deviation in visual contrast sensitivity (**A**, $P = 0.020$) and examination duration (**B**, $P = 0.003$) were observed across all participants ($n = 74$). Similar associations were observed when the analysis was limited to only the at-risk individuals (SCD and MCI participants; $n = 36$), including significant associations between temporal lobe volume and mean deviation (**C**, $P = 0.017$) and examination duration (**D**, $P = 0.011$). Note that examination duration (indicated as the natural log of seconds needed to complete the examination) is a measure of contrast sensitivity performance as the test is iterative and those with poorer contrast sensitivity take longer on the examination, while lower mean deviation scores represent poorer contrast sensitivity performance. **A** and **B** include 31 CN (blue circles), 20 SCD (green triangles), 16 MCI (yellow squares), and 7 AD (red diamonds); **C** and **D** include 20 SCD (green triangles) and 16 MCI (yellow squares).

easy-to-administer biomarker for Alzheimer's disease-related pathological changes.

Numerous studies have shown visual system dysfunction in patients with Alzheimer's disease and MCI (Albers *et al.*, 2015). The most consistent findings are a reduced retinal nerve fibre layer thickness in MCI and Alzheimer's disease (Coppola *et al.*, 2015). Fewer studies have addressed changes in retinal function, but deficits in visual evoked potential, colour vision and other changes have been observed (Frost *et al.*, 2010; Albers *et al.*, 2015). The findings in this study add to the long literature on contrast sensitivity deficits in Alzheimer's disease (Cronin-Golomb *et al.*, 1991; Cormack *et al.*, 2000; Crow *et al.*, 2003; Risacher *et al.*, 2013; Valenti, 2013; Fischer *et al.*, 2016; Polo *et al.*, 2017; Ward *et al.*, 2018), by linking visual dysfunction not only with clinical status but also with the underlying proteinopathies thought to cause Alzheimer's disease, thereby suggesting that these relationships may be potential underlying biological causes for previously observed deficits in contrast sensitivity in those with or at risk for Alzheimer's disease.

The underlying cause of deficits observed in visual system function and structure in MCI and Alzheimer's disease is unknown. However, changes in both the retina and brain could underlie some of these deficits. Recently, a number of studies have suggested local accumulation of amyloid-beta and tau deposits in the retina, both in animal models and post-mortem tissue (Koronyo-Hamaoui *et al.*, 2011; Chiasseu *et al.*, 2017; Koronyo *et al.*, 2017; den Haan *et al.*, 2018; Grimaldi *et al.*, 2018). A previous study in an Alzheimer's disease animal model suggested

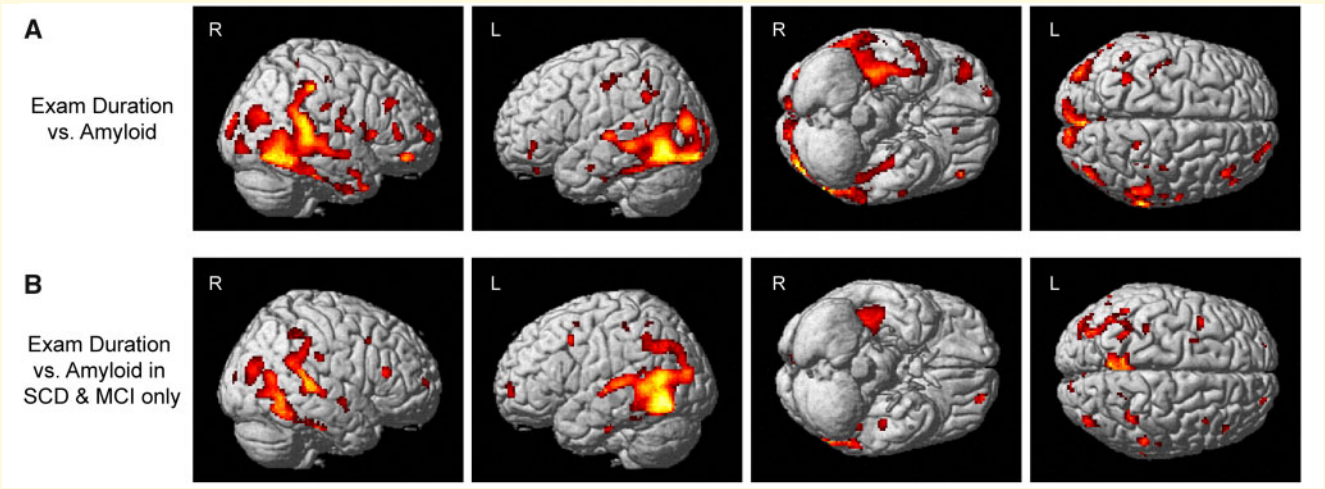

Figure 5 Visual contrast sensitivity is associated with voxel-wise cerebral amyloid deposition. On the voxel-wise analysis, significant associations between visual contrast sensitivity (examination duration) and amyloid deposition in the medial and lateral temporal and parietal lobes, as well as focal regions of the occipital and frontal lobes, were observed both (**A**) across all participants ($n = 74$; 31 CN, 20 SCD, 16 MCI, 7 AD) or (**B**) SCD and MCI individuals only ($n = 36$). Note that examination duration (indicated as the natural log of seconds needed to complete the examination) is a measure of contrast sensitivity performance as the test is iterative and those with poorer contrast sensitivity take longer on the examination, while lower mean deviation scores represent poorer contrast sensitivity performance. Both analyses are displayed at a voxel-wise threshold of *P*-value <0.05 (family-wise error correction for multiple comparisons) and minimum cluster size (k) = 10 voxels.

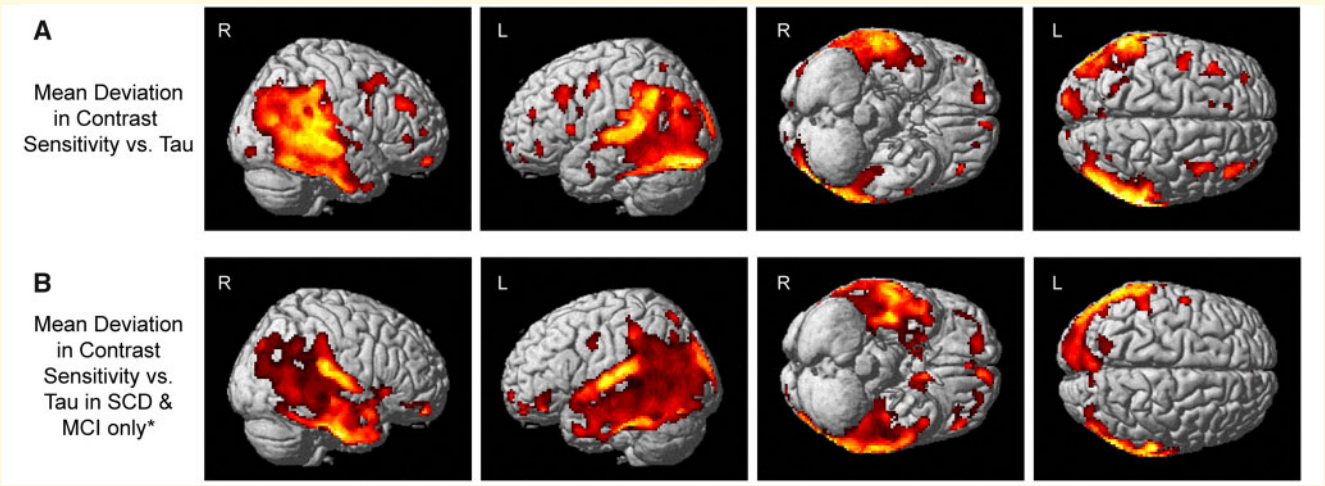

Figure 6 Visual contrast sensitivity is associated with voxel-wise cerebral tau deposition. Significant associations between mean deviation in visual contrast sensitivity and tau deposition in the lateral and medial temporal and parietal lobes, as well as focal regions of the occipital and frontal lobes, were observed both (**A**) across all participants ($n = 46$; 23 CN, 12 SCD, 9 MCI, 2 AD) or (**B**) SCD and MCI individuals only ($n = 21$). The full sample analysis (**A**) is displayed at a voxel-wise threshold of $P < 0.05$ [family-wise error (FWE) correction for multiple comparisons] and minimum cluster size (k) = 10 voxels. Note that lower mean deviation scores represent poorer contrast sensitivity performance. *The SCD and MCI participants only sample (**B**) is displayed at a cluster-wise threshold of *P*-value <0.05 (FWE correction for multiple comparisons), which is equivalent to *P*-value <0.001 (uncorrected) and minimum cluster size (k) = 400 voxels.

that amyloid accumulation in the retina occurs simultaneously with amyloid accumulation in the brain (Koronyo-Hamaoui *et al.*, 2011). In fact, a recent protocol to detect these deposits *in vivo* has been recently reported and reflects an exciting potential area for the biomarker detection of Alzheimer's disease (Klunk *et al.*, 2015). Furthermore, previous studies have suggested local dysfunction, neuroinflammation and loss of retinal ganglion cells associated with tau aggregation in an animal model (Chiasseu *et al.*, 2017; Grimaldi *et al.*, 2018). Thus, the visual contrast sensitivity deficits that we observed in the present study could be due to local degeneration of

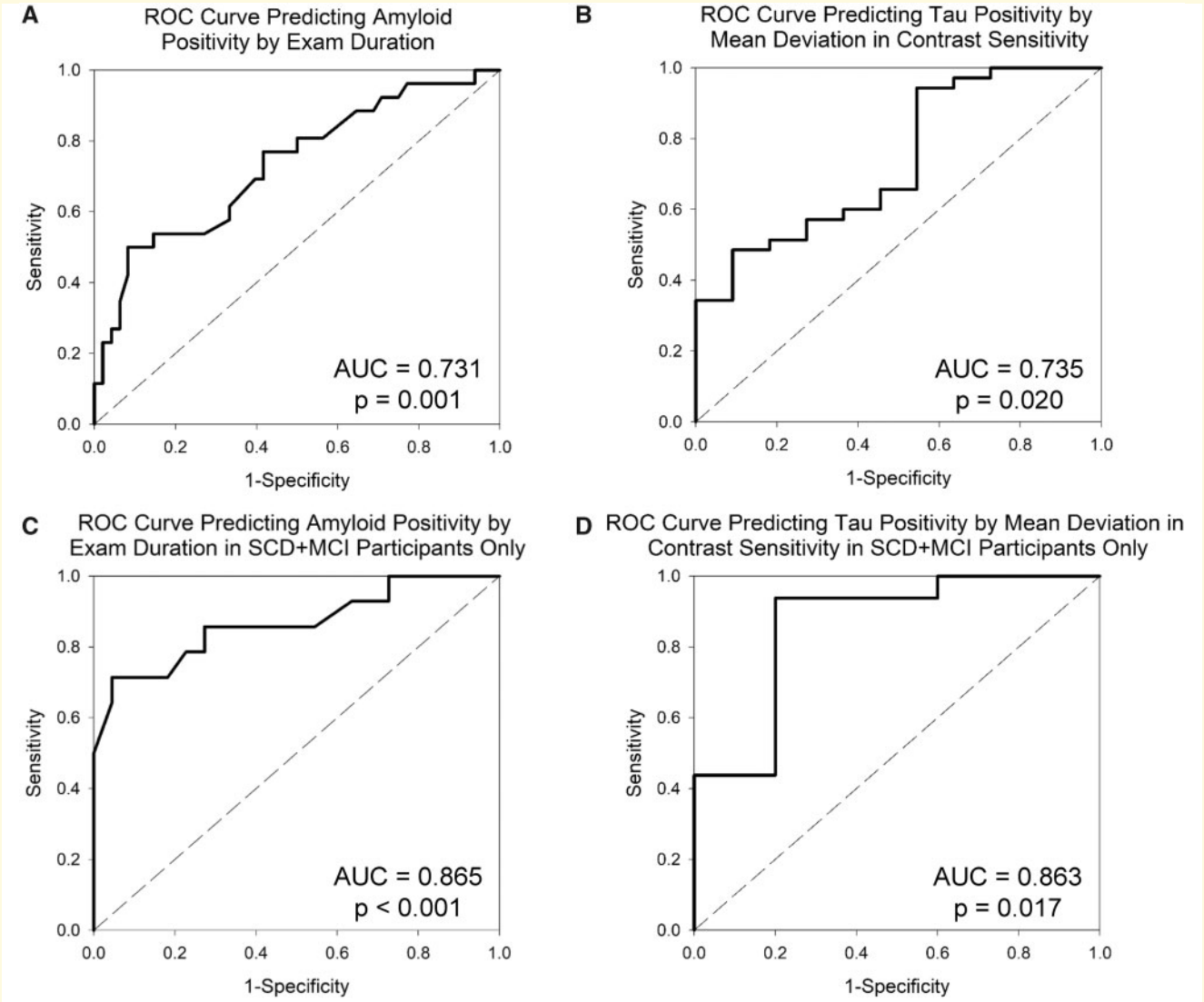

Figure 7 Receiver operating characteristic (ROC) curves for predicting amyloid and tau positivity by visual contrast sensitivity. Visual contrast sensitivity (examination duration) significantly predicted amyloid positivity (defined as cortical Centiloid value ≥21.02) in the full sample (**A**; $n = 74$; AUC = 0.731, $P = 0.001$). In addition, visual contrast sensitivity (mean deviation) predicted tau positivity, defined as assignment to Braak stage ≥4 (Schwarz *et al.*, 2018), in the full sample (**B**; $n = 46$; AUC = 0.735, $P = 0.020$). In SCD and MCI participants only, similar patterns were seen with examination duration predicting amyloid positivity (**C**; $n = 36$; AUC = 0.865, $P < 0.001$) and mean deviation-predicted tau positivity (**D**; $n = 21$; AUC = 0.863, $P = 0.017$). AUC: area under the curve.

retinal neuronal cells, including the retinal ganglion cells, due to the accumulation of amyloid and tau pathology.

Alternatively, amyloid and tau accumulation in the brain may also potentially underlie the observed changes in contrast sensitivity. The associations of contrast sensitivity dysfunction with amyloid were strongest in posterior regions of the brain, most especially the occipital lobe. Although this area is not considered to be highly impacted early in Alzheimer's disease, amyloid accumulation does occur in the occipital lobe (Thal *et al.*, 2002). These findings may suggest that at least part of the contrast sensitivity deficits could be due to central amyloid accumulation. Furthermore, the stereotypical progression of tau deposition beyond Braak stage 3 highly overlaps with the ventral visual stream and other visual association areas (Braak *et al.*, 2006). Again, tau deposition and associated neurodegeneration in these regions may underlie at least part of the observed changes in visual contrast sensitivity performance. Future studies with longitudinal FDT and neuroimaging, as well as visual studies in animal models of Alzheimer's disease, may help us to better understand the underlying pathology causing the observed changes in visual contrast sensitivity.

This study has a few limitations. Although by far the largest sample in a study of this type, the sample size is relatively modest. In addition, the study is cross-sectional. Future studies in a larger sample with longitudinal visual examinations, neuroimaging and clinical follow-up are warranted. The sample used in this analysis excludes individuals with primary open-angle glaucoma, macular degeneration and diabetic retinopathy, which are relatively common in aging populations. Future studies testing this tool in mixed samples of those with and without concurrent eye disease would be needed to demonstrate validity across a more clinically diverse set of individuals. However, the current data suggest that, in this population, visual contrast sensitivity on FDT is a good screening biomarker for the presence of Alzheimer's disease pathophysiology.

In sum, visual contrast sensitivity measures were strongly associated with the presence of cerebral amyloid and tau deposition. The findings suggest that visual contrast sensitivity should be explored further as an inexpensive, non-invasive and easy-to-administer tool for screening older adults for the presence of Alzheimer's disease pathology, especially when combined with other risk factors.

Acknowledgements

The authors thank Karmen K. Yoder, Gary D. Hutchins, James W. Fletcher, Aaron Vosmeier, Rachael Deardorff, Bradley Glazier, Kala Hall, Lili Kyurkchiyska, Evan Finley, Yolanda Graham-Dotson, Steve Brown, Trina Bird, Linda Morgan, Michele Spriggs, Heather Polson, Wendy Territo, Michelle Beal and Devon Mackay for their contributions to this work. They also thank Avid Radiopharmaceuticals, a subsidiary of Eli Lilly for the provision of the precursor for flortaucipir and permission to cross-reference their IND for AV1451 tracer manufacturing, which was performed by PETNET of Indiana in partnership with the Indiana University Department of Radiology and Imaging Sciences.

Funding

This work was supported by the National Institute on Aging (K01 AG049050, R01 AG061788, R01 AG19771 and P30 AG10133), a New Vision Award through Donors Cure Foundation, the Alzheimer's Association, the Indiana University Health-Indiana University School of Medicine Strategic Research Initiative and the Indiana Clinical and Translational Sciences Institute (CTSI). Part of this research was also supported in part by Lilly Endowment, Inc., through its support for the Indiana University Pervasive Technology Institute, and in part by the Indiana METACyt Initiative. The Indiana METACyt Initiative at Indiana University was also supported in part by Lilly Endowment, Inc. This material is based upon work supported by the National Science Foundation under grant no. CNS-0521433.

Competing interests

The authors report no competing interests or conflicts of interest.

References

Albers MW, Gilmore GC, Kaye J, Murphy C, Wingfield A, Bennett DA, et al. At the interface of sensory and motor dysfunctions and Alzheimer's disease. Alzheimers Dement 2015; 11: 70–98.

Anderson AJ, Johnson CA. Frequency-doubling technology perimetry. Ophthalmol Clin North Am 2003; 16: 213–25.

Alzheimer's Association. Alzheimer's disease facts and figures. Alzheimers Dement 2019; 15: 321–87.

Braak H, Alafuzoff I, Arzberger T, Kretzschmar H, Del Tredici K. Staging of Alzheimer disease-associated neurofibrillary pathology using paraffin sections and immunocytochemistry. Acta Neuropathol 2006; 112: 389–404.

Chiasseu M, Alarcon-Martinez L, Belforte N, Quintero H, Dotigny F, Destroismaisons L, et al. Tau accumulation in the retina promotes early neuronal dysfunction and precedes brain pathology in a mouse model of Alzheimer's disease. Mol Neurodegener 2017; 12: 58.

Coppola G, Di Renzo A, Ziccardi L, Martelli F, Fadda A, Manni G, et al. Optical coherence tomography in Alzheimer's disease: a meta-analysis. PLoS One 2015; 10: e0134750.

Cormack FK, Tovee M, Ballard C. Contrast sensitivity and visual acuity in patients with Alzheimer's disease. Int J Geriatr Psychiatry 2000; 15: 614–20.

Cronin-Golomb A, Corkin S, Rizzo JF, Cohen J, Growdon JH, Banks KS. Visual dysfunction in Alzheimer's disease: relation to normal aging. Ann Neurol 1991; 29: 41–52.

Crow RW, Levin LB, LaBree L, Rubin R, Feldon SE. Sweep visual evoked potential evaluation of contrast sensitivity in Alzheimer's dementia. Invest Ophthalmol Vis Sci 2003; 44: 875–8.

den Haan J, Morrema THJ, Verbraak FD, de Boer JF, Scheltens P, Rozemuller AJ, et al. Amyloid-beta and phosphorylated tau in post-mortem Alzheimer's disease retinas. Acta Neuropathol Commun 2018; 6: 147.

Fischer ME, Cruickshanks KJ, Schubert CR, Pinto AA, Carlsson CM, Klein BE, et al. Age-related sensory impairments and risk of cognitive impairment. J Am Geriatr Soc 2016; 64: 1981–7.

Frost S, Martins RN, Kanagasingam Y. Ocular biomarkers for early detection of Alzheimer's disease. J Alzheimers Dis 2010; 22: 1–16.

Grimaldi A, Brighi C, Peruzzi G, Ragozzino D, Bonanni V, Limatola C, et al. Inflammation, neurodegeneration and protein aggregation in the retina as ocular biomarkers for Alzheimer's disease in the 3xTg-AD mouse model. Cell Death Dis 2018; 9: 685.

Haan JD, van de Kreeke JA, Konijnenberg E, Kate MT, Braber AD, Barkhof F, et al. Retinal thickness as a potential biomarker in patients with amyloid-proven early- and late-onset Alzheimer's disease. Alzheimers Dement (Amst) 2019; 11: 463–71.

Jack CR Jr, Bennett DA, Blennow K, Carrillo MC, Dunn B, Haeberlein SB, et al. NIA-AA Research Framework: Toward a biological definition of Alzheimer's disease. Alzheimers Dement 2018; 14: 535–62.

Jessen F, Amariglio RE, van Boxtel M, Breteler M, Ceccaldi M, Chételat G, et al. A conceptual framework for research on subjective cognitive decline in preclinical Alzheimer's disease. Alzheimers Dement 2014; 10: 844–52.

Jung NY, Han JC, Ong YT, Cheung CY, Chen CP, Wong TY, et al. Retinal microvasculature changes in amyloid-negative subcortical

vascular cognitive impairment compared to amyloid-positive Alzheimer's disease. J Neurol Sci 2019; 396: 94–101.

Klunk WE, Koeppe RA, Price JC, Benzinger TL, Devous MD Sr, Jagust WJ, et al. The Centiloid Project: standardizing quantitative amyloid plaque estimation by PET. Alzheimers Dement 2015; 11: 1–15.e1–4.

Koronyo Y, Biggs D, Barron E, Boyer DS, Pearlman JA, Au WJ, et al. Retinal amyloid pathology and proof-of-concept imaging trial in Alzheimer's disease. JCI Insight 2017; 2: e93621.

Koronyo Y, Salumbides BC, Black KL, Koronyo-Hamaoui M. Alzheimer's disease in the retina: imaging retinal abeta plaques for early diagnosis and therapy assessment. Neurodegenerative Dis 2012; 10: 285–93.

Koronyo-Hamaoui M, Koronyo Y, Ljubimov AV, Miller CA, Ko MK, Black KL, et al. Identification of amyloid plaques in retinas from Alzheimer's patients and noninvasive in vivo optical imaging of retinal plaques in a mouse model. Neuroimage 2011; 54 (Suppl 1): S204–17.

McKendrick AM, Turpin A. Advantages of terminating Zippy Estimation by Sequential Testing (ZEST) with dynamic criteria for white-on-white perimetry. Optom Vis Sci 2005; 82: 981–7.

McKhann GM, Knopman DS, Chertkow H, Hyman BT, Jack CR Jr, Kawas CH, et al. The diagnosis of dementia due to Alzheimer's disease: recommendations from the National Institute on Aging-Alzheimer's Association workgroups on diagnostic guidelines for Alzheimer's disease. Alzheimers Dement 2011; 7: 263–9.

Navitsky M, Joshi AD, Kennedy I, Klunk WE, Rowe CC, Wong DF, et al. Standardization of amyloid quantitation with florbetapir standardized uptake value ratios to the Centiloid scale. Alzheimers Dement 2018; 14: 1565–71.

Petersen RC. Mild cognitive impairment as a diagnostic entity. J Intern Med 2004; 256: 183–94.

Polo V, Rodrigo MJ, Garcia-Martin E, Otin S, Larrosa JM, Fuertes MI, et al. Visual dysfunction and its correlation with retinal changes in patients with Alzheimer's disease. Eye (Lond) 2017; 31: 1034–41.

Rattanabannakit C, Risacher SL, Gao S, Lane KA, Brown SA, McDonald BC, et al. The Cognitive Change Index as a measure of self and informant perception of cognitive decline: relation to neuropsychological tests. J Alzheimers Dis 2016; 51: 1145–55.

Risacher SL, Tallman EF, West JD, Yoder KK, Hutchins GD, Fletcher JW, et al. Olfactory identification in subjective cognitive decline and mild cognitive impairment: association with tau but not amyloid positron emission tomography. Alzheimers Dement (Amst) 2017; 9: 57–66.

Risacher SL, Wudunn D, Pepin SM, MaGee TR, McDonald BC, Flashman LA, et al. Visual contrast sensitivity in Alzheimer's disease, mild cognitive impairment, and older adults with cognitive complaints. Neurobiol Aging 2013; 34: 1133–44.

Rowe CC, Dore V, Jones G, Baxendale D, Mulligan RS, Bullich S, et al. (18)F-Florbetaben PET beta-amyloid binding expressed in Centiloids. Eur J Nucl Med Mol Imaging 2017; 44: 2053–9.

Santos CY, Johnson LN, Sinoff SE, Festa EK, Heindel WC, Snyder PJ. Change in retinal structural anatomy during the preclinical stage of Alzheimer's disease. Alzheimers Dement (Amst) 2018; 10: 196–209.

Saykin AJ, Wishart HA, Rabin LA, Santulli RB, Flashman LA, West JD, et al. Older adults with cognitive complaints show brain atrophy similar to that of amnestic MCI. Neurology 2006; 67: 834–42.

Schwarz AJ, Shcherbinin S, Slieker LJ, Risacher SL, Charil A, Irizarry MC, et alet al. Topographic staging of tau positron emission tomography images. Alzheimer's Disease Neuroimaging Initiative 2018; 10: 221–31.

Snyder PJ, Johnson LN, Lim YY, Santos CY, Alber J, Maruff P, et al. Nonvascular retinal imaging markers of preclinical Alzheimer's disease. Alzheimers Dement (Amst) 2016; 4: 169–78.

Sperling RA, Aisen PS, Beckett LA, Bennett DA, Craft S, Fagan AM, et al. Toward defining the preclinical stages of Alzheimer's disease: recommendations from the National Institute on Aging-Alzheimer's Association workgroups on diagnostic guidelines for Alzheimer's disease. Alzheimers Dement 2011; 7: 280–92.

Teipel S, Drzezga A, Grothe MJ, Barthel H, Chetelat G, Schuff N, et al. Multimodal imaging in Alzheimer's disease: validity and usefulness for early detection. Lancet Neurol 2015; 14: 1037–53.

Thal DR, Rub U, Orantes M, Braak H. Phases of A beta-deposition in the human brain and its relevance for the development of AD. Neurology 2002; 58: 1791–800.

Trzepacz PT, Hochstetler H, Wang S, Walker B, Saykin AJ; for the Alzheimer's Disease Neuroimaging Initiative. Alzheimer's disease neuroimaging I. Relationship between the Montreal Cognitive Assessment and Mini-Mental State Examination for assessment of mild cognitive impairment in older adults. BMC Geriatr 2015; 15: 107.

Turpin A, McKendrick AM, Johnson CA, Vingrys AJ. Properties of perimetric threshold estimates from full threshold, ZEST, and SITA-like strategies, as determined by computer simulation. Invest Ophthalmol Vis Sci 2003; 44: 4787–95.

Valenti DA. Alzheimer's disease: screening biomarkers using frequency doubling technology visual field. ISRN Neurol 2013; 2013: 1–9.

van de Kreeke JA, Nguyen HT, den Haan J, Konijnenberg E, Tomassen J, den Braber A, et al. Retinal layer thickness in preclinical Alzheimer's disease. Acta Ophthalmol 2019; 97: 798–804.

van de Kreeke JA, Nguyen HT, Konijnenberg E, Tomassen J, den Braber A, Ten Kate M, et al. Optical coherence tomography angiography in preclinical Alzheimer's disease. Br J Ophthalmol 2020; 104: 157–61.

Ward ME, Gelfand JM, Lui LY, Ou Y, Green AJ, Stone K, et al. Reduced contrast sensitivity among older women is associated with increased risk of cognitive impairment. Ann Neurol 2018; 83: 730–8.

Weintraub S, Besser L, Dodge HH, Teylan M, Ferris S, Goldstein FC, et al. Version 3 of the Alzheimer Disease Centers' neuropsychological test battery in the uniform data set (UDS). Alzheimer Dis Assoc Disord 2018; 32: 10–7.

Williams EA, McGuone D, Frosch MP, Hyman BT, Laver N, Stemmer-Rachamimov A. Absence of Alzheimer disease neuropathologic changes in eyes of subjects with Alzheimer disease. J Neuropathol Exp Neurol 2017; 76: 376–83.

Zeppieri M, Johnson CA. Frequency Doubling Technology (FDT) Perimetry. Imaging and Perimetry Society. http://webeye.ophth.uiowa.edu/ips/PerimetryHistory/FDP/, 2008.